

10 The measurement of wavelet parameters from digital seismograms

Commonly used wavelet parameters

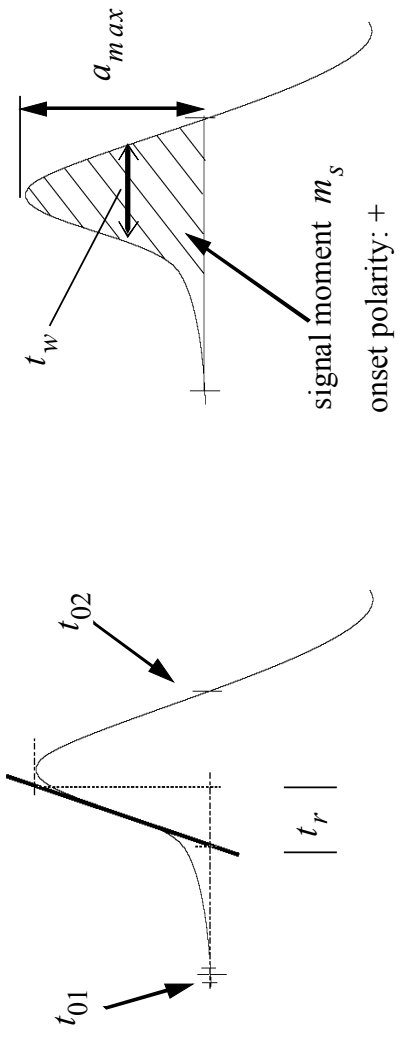


Fig. 10.1 Commonly determined signal parameters such as onset time t_{01} , onset polarity, amplitude a_{max} , rise time t_r , pulse width t_w or time of zero crossing t_{02} signal moment m_s .

Wavelet parameters can be severely affected by the properties of seismic recording systems!!!

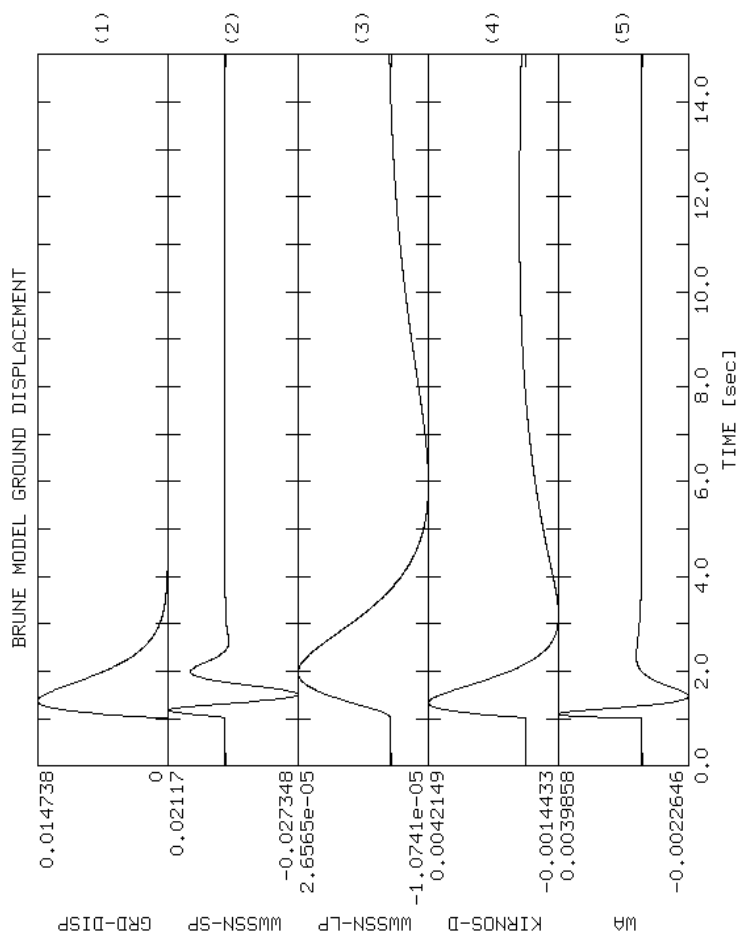


Fig. 10.2 Waveform distortion of a synthetic ground displacement signal (top trace) by standard seismograph systems (traces 2-5). Displayed in traces 2 to trace 5 are the output signals of simulated WWSSN-SP, WWSSN-LP, KIRNOS, and a Wood-Anderson instrument for the synthetic input signal shown in trace 1.

10.2 The properties of seismic onsets

Context: earthquake location, focal mechanisms, source modelling (friction law), traveltime tomography.

Qualitative description: impulsive, emergent, strong or weak.

Quantitative description: based on the order of discontinuity at the signal front of a causal signal $f(t)$ ($f(t) = 0$ for $t < 0$).

Definition: The discontinuity of the signal front $t = 0$ is called an onset of order p , if $f^{(p)}(0+)$ is the first nonzero derivative.

Onset time (arrival time): $t = 0$

Onset polarity: sign of the discontinuity (+1 or -1)

Examples:

- a) unit step function $u(t)$ ($u(t) = 0$ for $t < 0$ and $u(t) = 1$ for $t \geq 0$) corresponds to an onset of order zero.
- b) The signal $f(t) = C t^a e^{(bt)} u(t)$ corresponds to an onset of order a . A special case of this signal for $a = 1$ is the Brune model far field source time function (Brune, 1970, 1971). It corresponds to an onset of order 1.

Onset distortion by seismometer systems

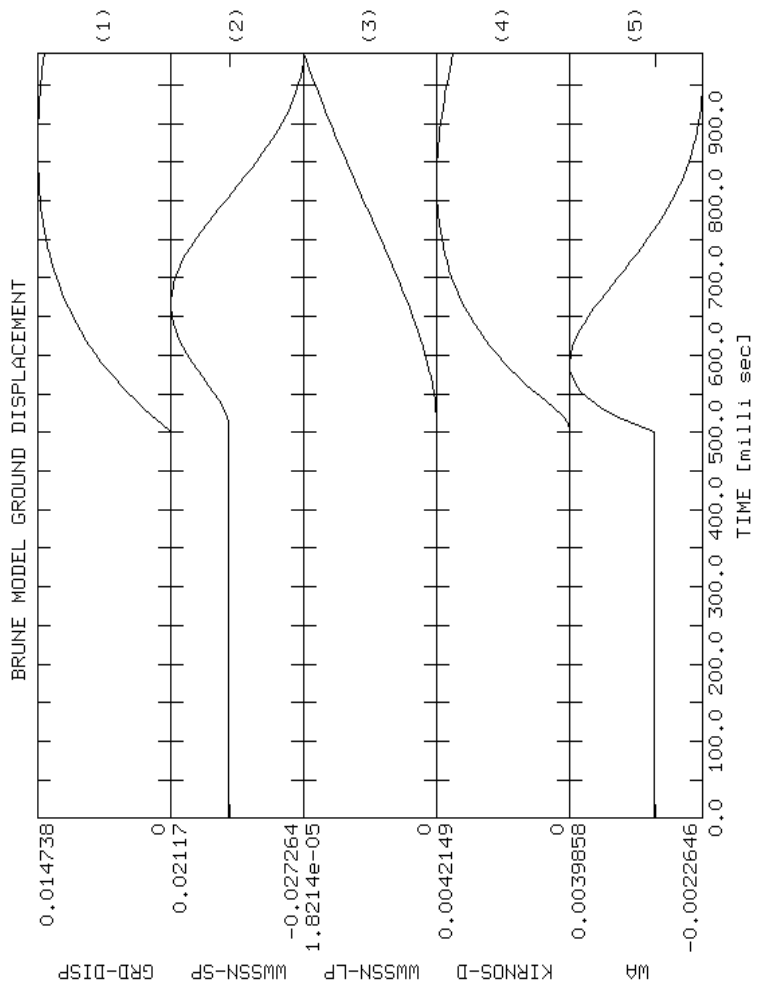


Fig. 10.11 Onset distortion of a far field Brune model ground displacement pulse (onset order 1, top trace) by standard seismograph systems (traces 2-5). Displayed in traces 2 to trace 5 are the output signals of simulated WWSSN-SP, WWSSN-LP, KIRNOS, and a Wood-Anderson instrument for the synthetic input signal shown in trace 1.

10.2.2 Onset order

Theoretical background: initial value theorem of the Laplace transform for causal functions
(unilateral Laplace transform)

Motivation for **bilateral** $L(f(t))$: different impulse response functions depending on ROC.
Relationship acausality and stability (IFT and acausality).

Benefits of **unilateral** $L(f(t))$ for **causal** systems: Relationship between onset distortions and
frequency domain properties of the seismic recording system.

Causality of functions implies symmetries for the corresponding integral transforms (Fourier,
Laplace, z). E. g. constraints on the types of attenuation laws permissible in nature (Aki and
Richards, 1980).

The unilateral Laplace transform

The unilateral Laplace transform of a causal function $f(t)$ ($f(t) = 0$ for $t < 0$) is defined as:

$$L_I[f(t)] = \int_{0+}^{\infty} f(t) e^{-st} dt$$

with the complex variable $s = \sigma + j\omega$. $L_I[f(t)]$ will be written as $F_I(s)$ to distinguish it from the two-sided Laplace transform defined in equation (2.25). The lower integration limit has to be interpreted as approaching zero from positive times.

Inverse transform

$$L_I^{-1}[F_I(s)] = f(t) = \frac{1}{2\pi j} \int_{\sigma-j\infty}^{\sigma+j\infty} F_I(s) e^{st} ds$$

Path of integration in ROC (for causal functions RHP),

Transform of a derivative: incorporation of initial values of the time function!

If $f(t)$ and $F_I(s)$ are a unilateral Laplace transform pair

$$\mathbf{L}_I[\dot{f}(t)] = sF_I(s) - f(0+)$$

with $f(0+)$ being the initial value of $f(t)$ ($\lim_{t \rightarrow 0^+} f(t)$ with the limit taken for positive times). Similarly, for n higher order derivatives, initial values of $f(t)$ and of its $n-1$ derivatives have to be incorporated

$$\mathbf{L}_I[f^{(n)}(t)] = s^n F_I(s) - \sum_{k=1}^n s^{n-k} \cdot f^{(k-1)}(0+)$$

With equation (10-16) the value $L_I[\dot{f}(t)]$ of for $s \rightarrow \infty$ becomes

$$\lim_{s \rightarrow \infty} L_I[\dot{f}(t)] = \lim_{s \rightarrow \infty} \int_{0^+}^{\infty} \dot{f}(t) e^{-st} dt$$

If $\dot{f}(t)$ does not contain impulses at the origin (which by the sifting properties of the delta function would always make the integral final), for causal functions only defined for $t > 0$, the value of the integral tends to zero for $s \rightarrow \infty$. Therefore

$$\lim_{s \rightarrow \infty} \int_{0^+}^{\infty} \dot{f}(t) e^{-st} dt = s F_I(s) - f(0^+) = 0$$

or

Initial value theorem (of the unilateral Laplace transform)

$$f(0^+) = \lim_{t \rightarrow 0} f(t) = \lim_{s \rightarrow \infty} s F_I(s) \quad (5-36)$$

“The high frequency limit of a frequency response function ($s \rightarrow j\omega$) will control the shape of a seismic onset $f(t)$ (for $t \rightarrow 0$ ”).

Seismic onset of order p : $f^{(p)}(0+) = f_p$ is the first non-zero derivative and $f^{(m)}(0+)$ $= 0$ for $m < p$. Combining the time derivative property (10-17) and the initial value theorem (10-21)

$$f^{(p)}(0+) = \lim_{t \rightarrow 0} f^{(p)}(t) = \lim_{s \rightarrow \infty} s^{p+1} F_I(s) = f_p$$

Dividing equation (10-21) by s^{p+1} we obtain

$$\lim_{s \rightarrow \infty} F_I(s) = \frac{f_p}{s^{p+1}}$$

Since $1/s^{p+1}$ is the Laplace transform of $(t^p / p!)$ $u(t)$ with $u(t)$ being the unit step function (Oppenheim and Willsky, 1983), the waveform of the onset is approximately

$$f(t) \approx \frac{f_p}{p!} \cdot t^p \quad \text{for } t = 0^+ \quad (\text{Seidl and Stammier, 1984}).$$

Special case: If for $s \rightarrow \inf$ the transfer function of the recording system is proportional to $s^{(p+1)}$ with p being an integer, the onset shape takes the particularly simple form of being proportional to t^p for $t \sim 0^+$.

Classical standardized seismometer-galvanometer systems:

$$T(s) = \frac{-\beta_L \cdot \prod_{k=1}^L (s - s_{0k})}{\alpha_N \cdot \prod_{k=1}^N (s - s_{pk})} = \frac{\beta_0 + \beta_1 s + \beta_2 s^2 + \dots + \beta_L s^L}{\alpha_0 + \alpha_1 s + \alpha_2 s^2 + \dots + \alpha_N s^N}$$

with N poles at the roots of the denominator polynomial, L zeroes at the roots of the numerator polynomial. For $s \rightarrow \inf$

$$\lim_{s \rightarrow \infty} T(s) \rightarrow \frac{\beta_L s^L}{\alpha_N s^N} = c \cdot s^{L-N}$$

Therefore the Laplace transform of a causal signal with onset order p recorded by a seismometer system with transfer function $T(s)$ becomes for $s \rightarrow \inf$

$$\lim_{s \rightarrow \infty} T(s) F_I(s) \approx c \cdot s^{L-N} \cdot \frac{f_p}{s^{p+1}}$$

Approximate wavelet shape at $t = 0+$

$$f(t) \approx \frac{c \cdot f_p}{(L - N + p)!} \cdot t^{N - L + p}$$

A recording system with a rational transfer function with N poles and L zeroes reduces the order of a onset and hence changes the initial slope of the onset by $N - L$.

Onset polarity

Approximate wavelet shape at $t = 0+$

$$f(t) \approx \frac{c \cdot f_p}{(L - N + p)!} \cdot t^{N - L + p}$$

Onset scaling factor ($(c f_p) / (L - N + p)!$) is independent of frequency!

No frequency dependent change in the onset polarity is possible for recording systems with rational transfer functions. The onset polarity is solely depending on the initial normalization of c (normally positive).

Filter properties and onset time

- Zero phase filters cause acausalities
- HF properties of a filter may cause apparent delay (Fig. 10.12).

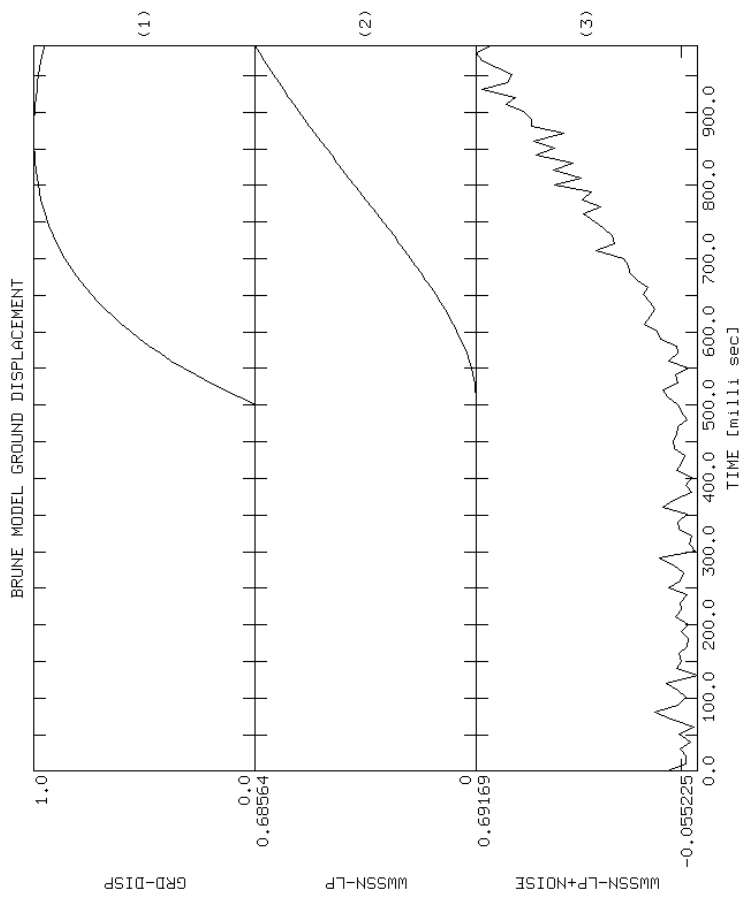


Fig. 10.12 Apparent onset delay caused by the change of the onset order. The top trace shows a synthetic seismic source signal (Brune, 1971) which is filtered by a WWSSN-LP system (second trace). In the bottom trace Gaussian noise has been superimposed to demonstrate the apparent onset delay.

Phase properties and delay times

Individual harmonic component

Input signal: $A \cdot \sin(\omega_0 \cdot t)$

Frequency response function: $T(j\omega) = |T(j\omega)| \cdot e^{j\Phi(\omega)}$

Filter output signal: $A \cdot |T(j\omega)| \cdot \sin(\omega_0 \cdot t + \Phi(\omega_0))$

The phase $\Phi(\omega)$ gives the amount by which the phase of a harmonic signal with frequency ω is advanced [in radians].

Phase delay $t_{ph}(\omega)$ in [s]

$$t_{ph}(\omega) = -\Phi(\omega) / \omega$$

A harmonic signal with frequency ω which is filtered with a frequency response $|T(j\omega)|e^{j\Phi(\omega)}$ is delayed by $t_{ph}(\omega) = -\Phi(\omega)/\omega$ seconds. For arbitrary signals the phase delay describes the delay of a single harmonic component.

Special case: $\Phi(\omega)$ is a linear function of frequency \rightarrow constant time shift (shifting theorem of the Fourier transform)

$$\text{Time-shifting filter: } T(j\omega) = |T(j\omega)| \cdot e^{j\Phi(\omega)} = e^{-j\omega a}$$

Here a is the delay introduced by the time shifting filter in seconds.

Group delay $t_{gr}(\omega)$:

$$t_{gr}(\omega) = -\frac{d}{d\omega}\Phi(\omega)$$

Delay of the signal envelope (or center of gravity) in the case of narrow-band signals.

Signal front delay t_{fr}

$$t_{fr} = \lim_{\omega \rightarrow \infty} \frac{-\Phi(\omega)}{\omega} = \lim_{\omega \rightarrow \infty} t_{ph}(\omega)$$

Delay of the onset time for broadband signals (here group delay and phase delay have no meaning).

Seismograph systems with rational transfer functions

The phase response function becomes constant for $\omega \rightarrow \infty$. Hence, for analog seismograph systems which can be described by rational transfer functions

$$t_{fr} = \lim_{\omega \rightarrow \infty} \frac{-\Phi(\omega)}{\omega} = \lim_{\omega \rightarrow \infty} \frac{const}{\omega} = 0 \quad (\text{Seidl and Stammller, 1984}).$$

At first glance: only apparent onset time delays caused by changes in the onset order of a seismic wavelet. Watch out in the context of simulation filtering of digital seismograms!

Delays and onset distortion in digital filters

WWSSN SP simulation from poles and zeroes using DFT

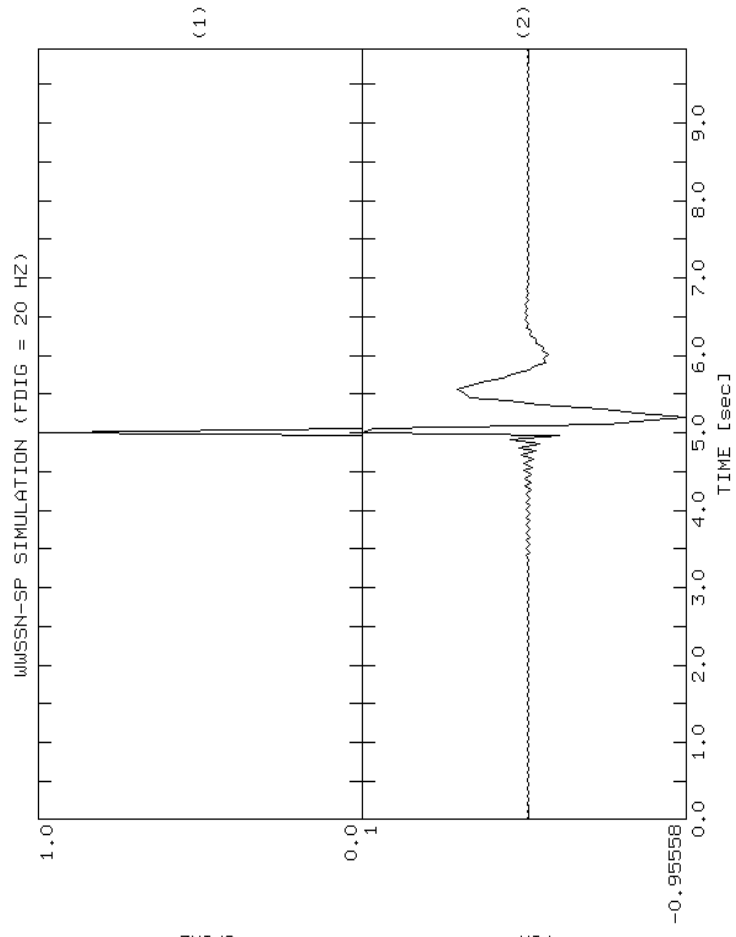


Fig. 10.13 Impulse response function for a WWSSN SP instrument, calculated for a sampling frequency of 20 Hz (bottom trace). The input impulse is displayed in the top trace. From the pole-zero positions of the transfer function the impulse response function should be completely causal.

A discrete impulse is not a spike!

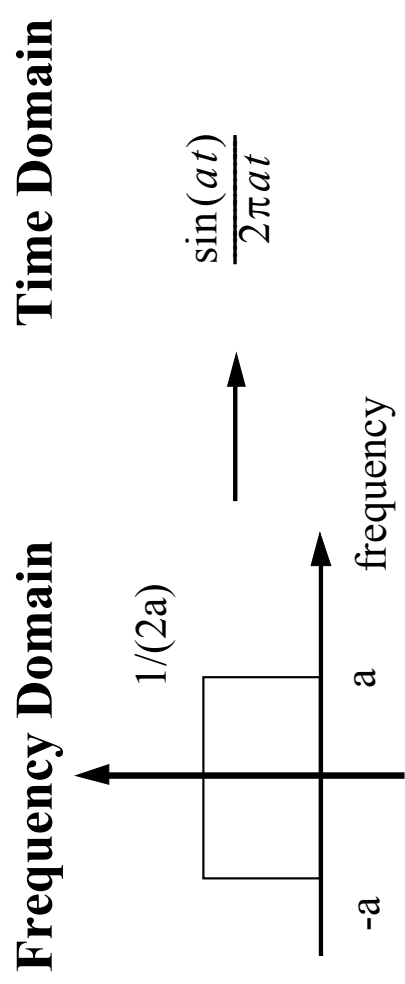


Fig. 10.14 Boxcar tapering window in frequency and time domain.

Time shifts by non-integer multiples of ΔT .

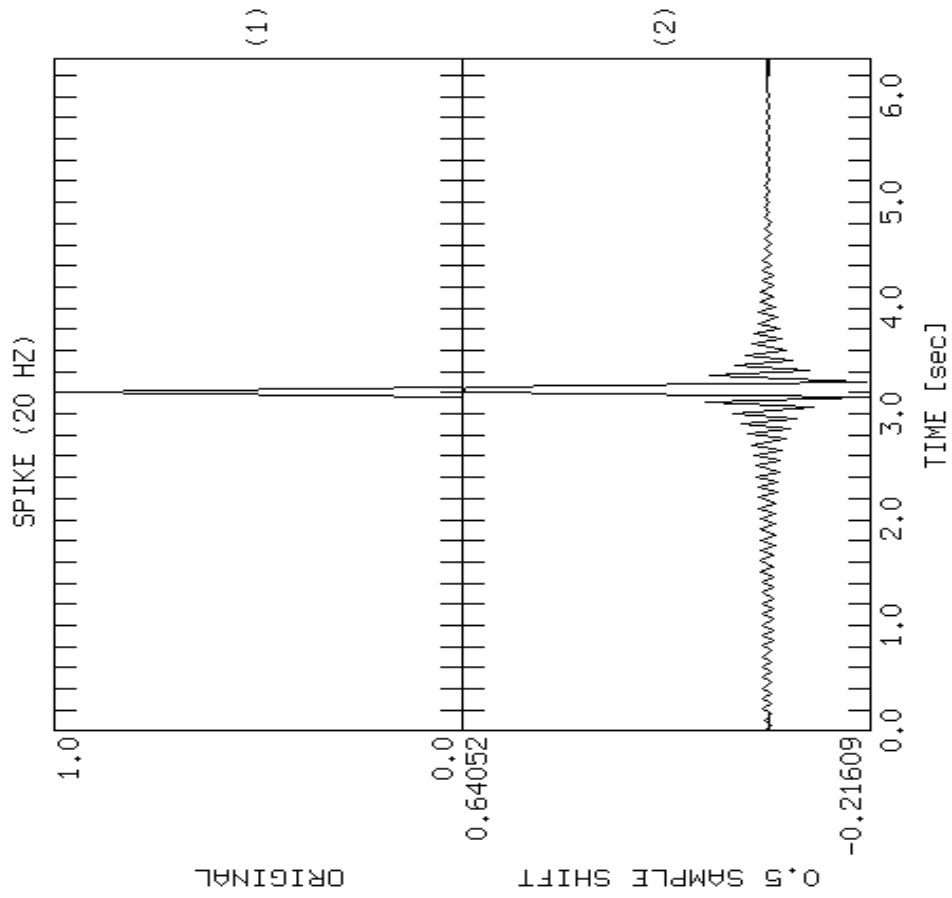


Fig. 10.15 Shifting a discrete impulse by a non-integer multiple of one sample. The lower trace was obtained by shifting the impulse in the upper trace by 0.5 samples.

Correction for phase delay at Nyquist frequency

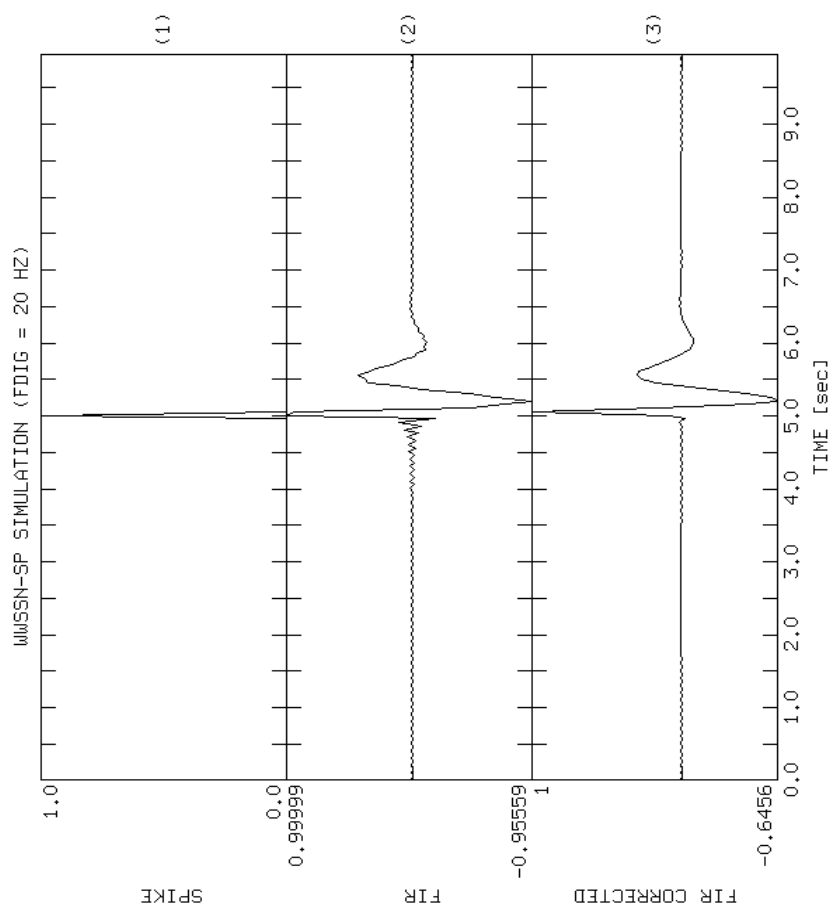


Fig. 10.16 Onset delay correction for the impulse response function shown in Fig. 10.13. The second trace shows the uncorrected impulse response. The bottom trace shows the result of shifting the second trace by the negative phase delay time at the Nyquist frequency.

Rise time and pulse duration

Context: Determination of source size and stress release. . .

Pulse rise time: interval between the intersection of the steepest rise of a wavelet with the zero level and peak pulse amplitude (Fig. 10.17, e.g. Gladwin and Stacey, 1974)

$$t_r = a_{max} / slope_{max}$$

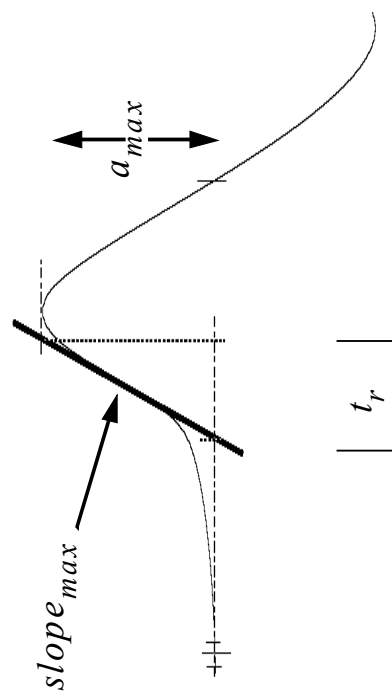


Fig. 10.17 Definition of pulse rise time t_r .

Problem 10.11 Calculate the rise time from the minimum to the maximum amplitude for a sinusoidal signal $A_0 \sin(\omega t)$.

Wavelet approximation by ramps of constant slope: rise time could be measured as pulse duration (from zero crossings) in the differentiated trace (Fig. 10.18).

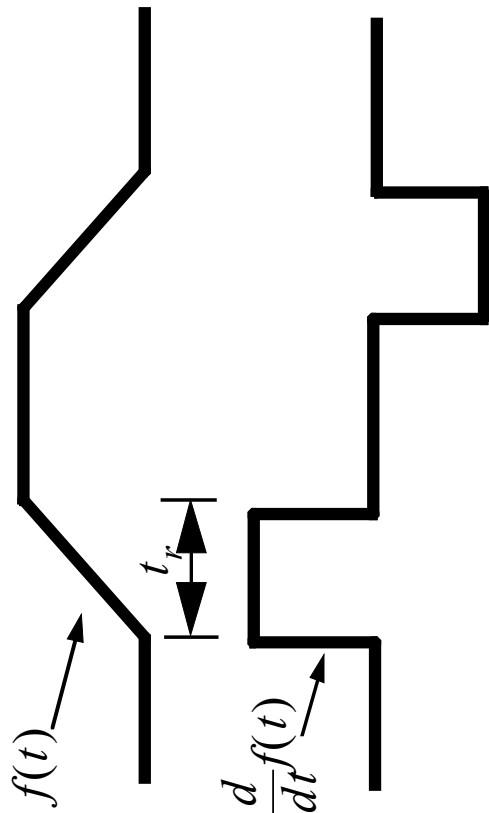


Fig. 10.18 Rise time t_r and pulse duration of the time derivative for ramp like wavelets.

Displacement step response functions for standard seismograph systems

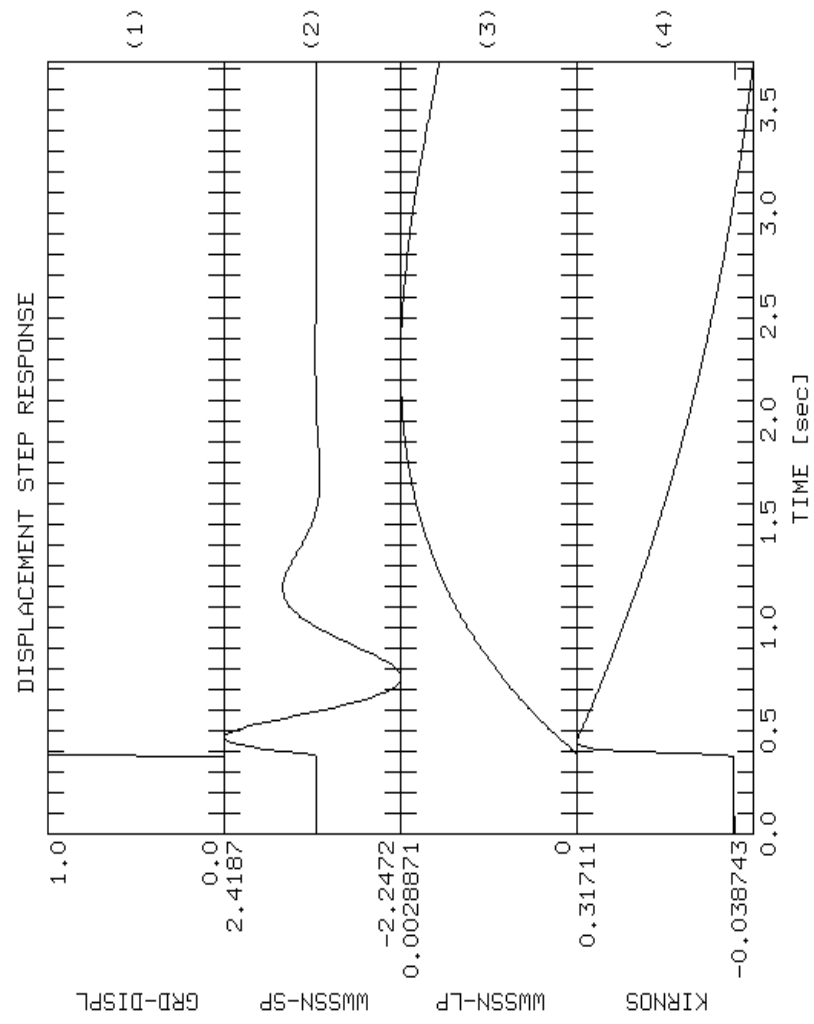


Fig. 10.19 Simulated displacement step response functions for commonly used standard seismograph systems.

Rise time for an ideal low pass filter.

Ideal Low Pass Filter
(frequency domain)

Impulse response
(time domain)

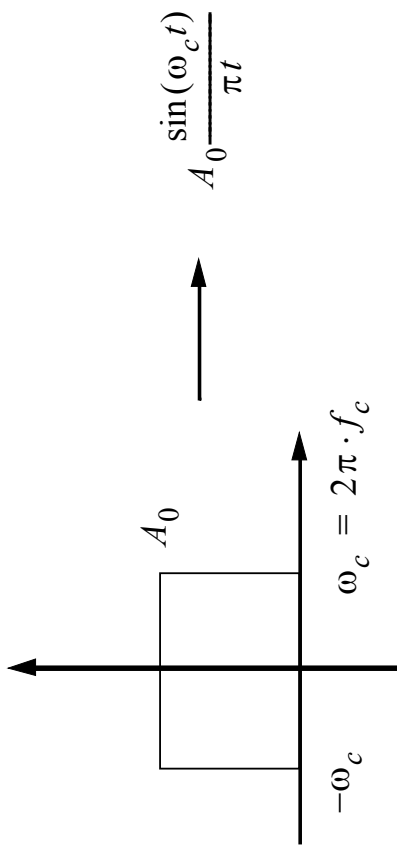


Fig. 10.20 Ideal low pass filter.

In this case, impulse and step response functions would be given by

$$A_0 \frac{\sin(\omega_c t)}{\pi t}$$

and

$$\frac{A_0}{2} + \frac{A_0}{\pi} \cdot \int_{-\infty}^t \frac{\sin(\omega_c \tau)}{\tau} d\tau = \frac{A_0}{2} \left(1 + \frac{2}{\pi} Si(\omega_c t) \right)$$

respectively (Papoulis, 1962). Here $Si(t)$ is the sine integral.

Evaluating these expressions for the maximum slope and the maximum amplitude yields according to (10-34) for the rise time

$$t_{r(idealLP)} = 1 / (2 \cdot f_c) \quad (\text{Papoulis, 1962}).$$

For a zero phase low pass filter with arbitrary spectral shape $A(\omega)$, the rise time becomes

$$t_r = \frac{A_0 2\pi}{\int_{-\infty}^{\infty} A(\omega) d\omega} \quad (\text{Papoulis, 1962})$$

Example

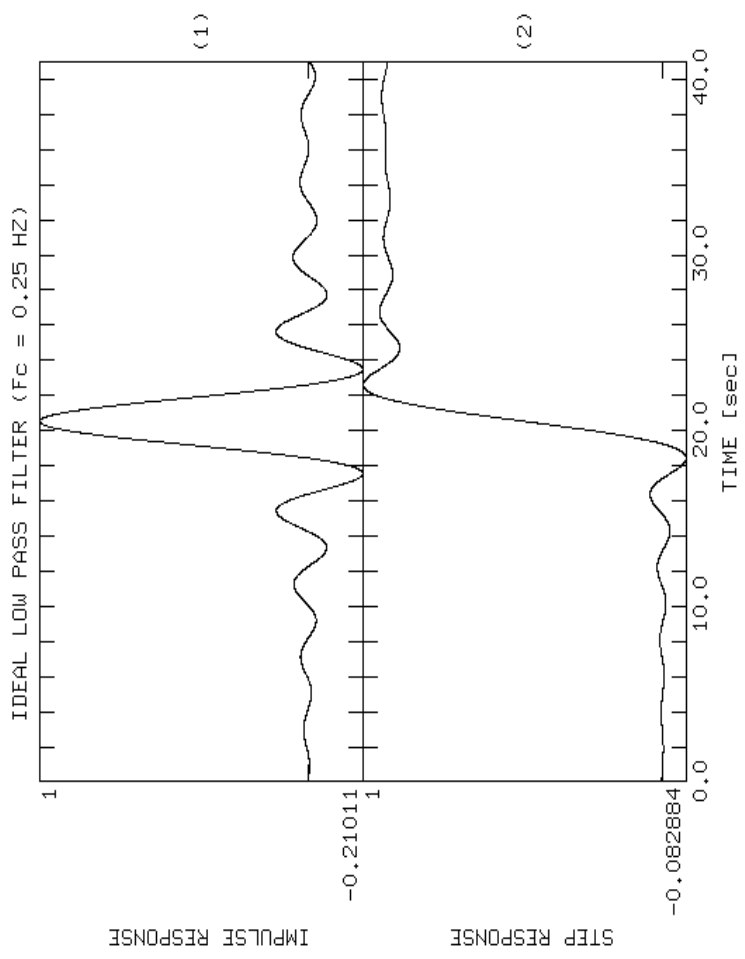


Fig. 10.21 Impulse and step response function for a boxcar lowpass filter with a rise time of 2 sec. The traces are shifted to the center of the plot for display purpose.

Note that expressions (10-37) and (10-38) are strictly valid only for zero phase low pass filters.

Problem 10.12 Calculate the impulse and step response functions for a causal and an acausal Butterworth LP filter with 8 poles and a corner frequency of 1 Hz using PITSA. Discuss time delays and the minimum detectable pulse duration and rise times for potential filter signals.

10.3 Signal moment

Seismic moment M_0 :

$$M_0 = \mu \cdot \bar{u} \cdot A$$

with \mathcal{O} being the shear modulus, \bar{u} being the average slip, and A being the fault area (Aki and Richards, 1980).

$$M_0 = C \cdot U(0)$$

with $U(0)$ being the spectral level of the farfield displacement pulse at frequency zero, G a constant factor containing the correction for radiation pattern, geometrical amplitude spreading, attenuation and the effects of the free surface.

From the definition of the Fourier transform in equation (2.8) we can see that $U(0)$ can be calculated in either the frequency or the time domain since

$$U(0) = \int_{-\infty}^{\infty} u(t) e^{-j2\pi ft} dt = \int_{-\infty}^{\infty} u(t) e^{-j2\pi 0t} dt = \int_{-\infty}^{\infty} u(t) dt = m_s$$

Hence, the spectral level at frequency zero $U(0)$ equals the pulse area in the time domain, a parameter commonly referred to as signal moment m_s (e.g. Seidl and Hellweg, 1988).

Signal moment determination without seismometer

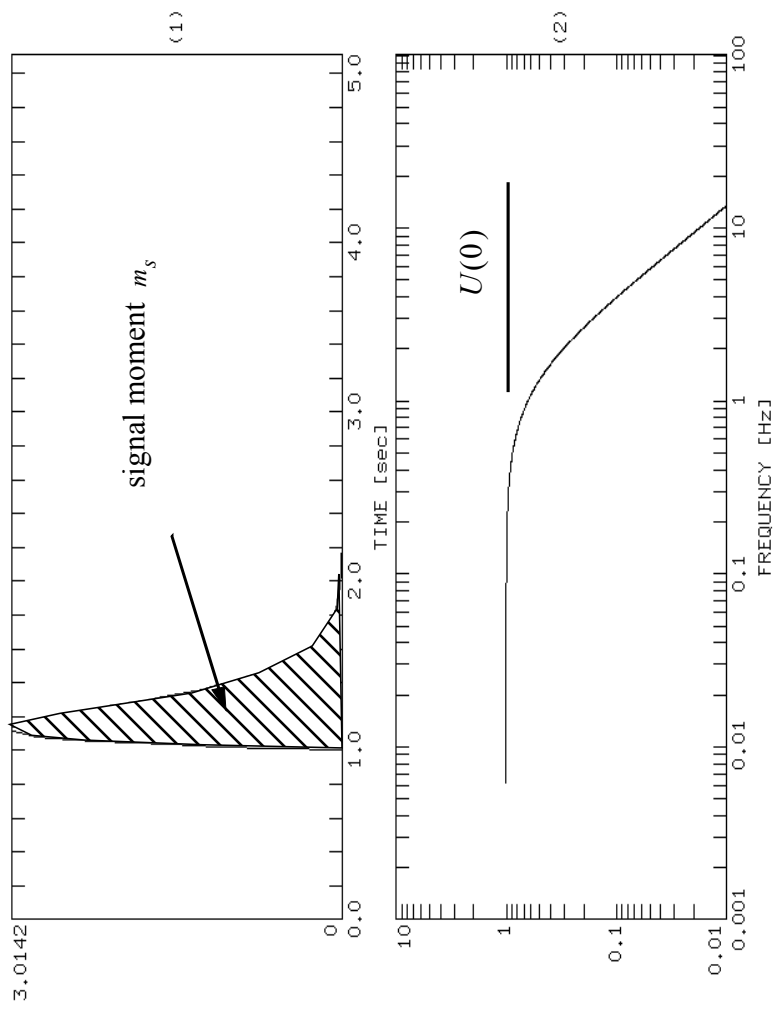


Fig. 10.22 The determination of signal moment m_s and $U(0)$.

Signal moment determination with seismometer

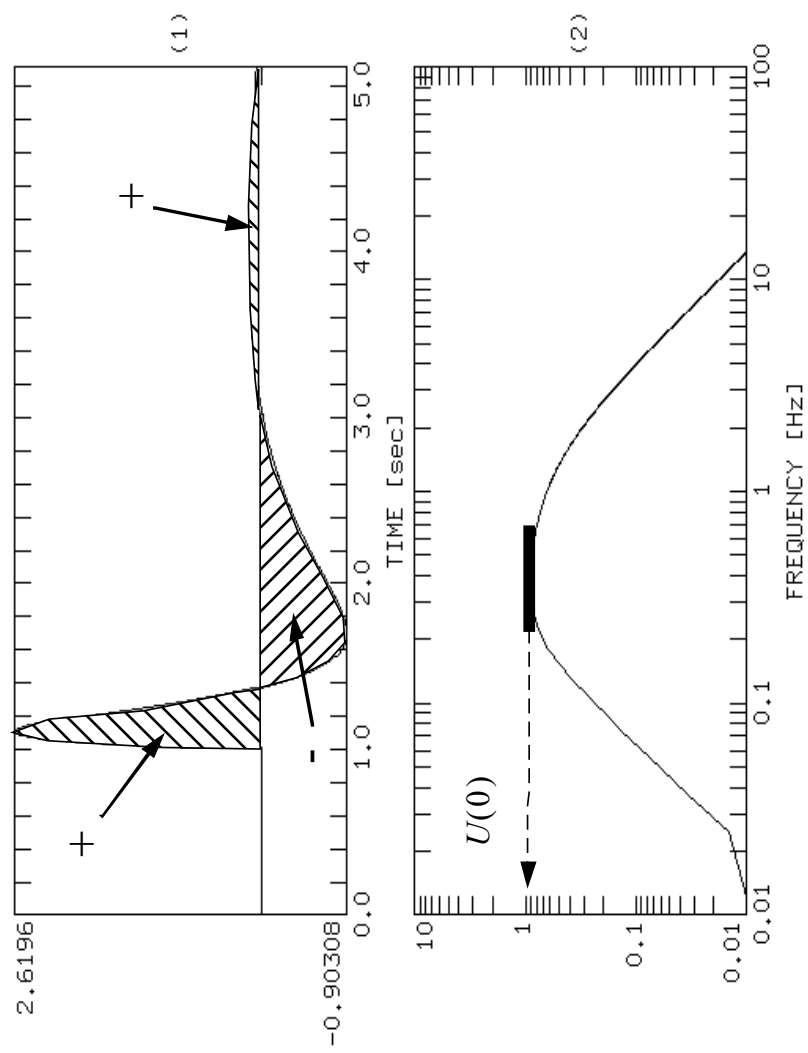


Fig. 10.23 Signal moment m_s and $U(0)$ for the signal from Fig. 10.22 as it would be recorded on a 5 sec displacement seismometer with a damping factor of 0.707.